Planetary interiors: Magnetic fields, Convection and Dynamo Theory 5. How numerical dynamo models are constructed and what they produce

Chris Jones, Department of Applied Mathematics
University of Leeds UK

FDEPS Lecture 5, Kyoto, 30th November 2017

UNIVERSITY OF LEEDS

Science & Technology Facilities Council

Section 5.

How numerical dynamo models are constructed and what they produce

5.1 Spherical geodynamo models

Spherical geometry Boussinesq dynamo models

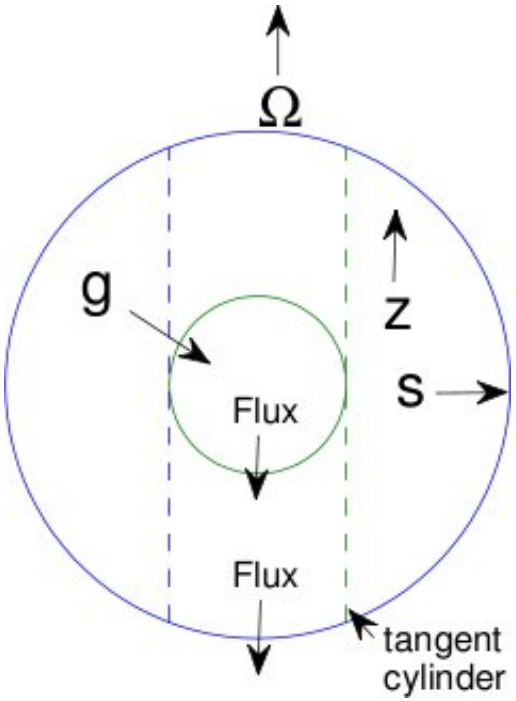

Model for the geodynamo.

Spherical shell rotating about z-axis. Gravity radially inward, $g = g_0 r$. Centrifugal acceleration small. Length scale d is gap-width from inner to outer boundary. Convection onsets outside tangent cylinder.

Tangent cylinder (TC) is imaginary cylinder touching the inner core. Convection columns inside the TC are divided.

Boussinesq fluid. Sometimes consider basal heating through the inner core boundary (ICB), sometimes internal heating.

Spherical dynamo equations

$$\frac{D\mathbf{u}}{Dt} + 2\boldsymbol{\Omega} \times \mathbf{u} = -\nabla p + \frac{1}{\rho}\mathbf{j} \times \mathbf{B} + \nu\nabla^2\mathbf{u} + g_0\alpha\theta\mathbf{r}, \qquad (5.1.1)$$

$$\frac{\partial \mathbf{B}}{\partial t} = \eta\nabla^2\mathbf{B} + \nabla \times (\mathbf{u} \times \mathbf{B}), \qquad (5.1.2)$$

$$\frac{\partial \theta}{\partial t} + \mathbf{u} \cdot \nabla\theta = \kappa\nabla^2\theta + \beta(r)u_r + H, \qquad (5.1.3)$$

$$\nabla \cdot \mathbf{B} = \nabla \cdot \mathbf{u} = 0, \qquad \mu\mathbf{j} = \nabla \times \mathbf{B}. \qquad (5.1.4, 5, 6)$$

$\beta(r)$ - Basic state temperature profile, H is heat source in the core. No-slip and stress-free boundaries considered, but assume $\theta = 0$ there.

Basic state in dynamo models

Basic state temperature satisfies

$$\kappa \nabla^2 \bar{T} + H = 0, \qquad \kappa \frac{1}{r^2} \frac{d}{dr} r^2 \frac{d\bar{T}}{dr} + H = 0, \tag{5.1.7}$$

so

$$\bar{T} = C_1 + \frac{C_2}{r} - \frac{Hr^2}{6\kappa} \tag{5.1.8}$$

where C_1 and C_2 are determined by the boundary conditions on T, e.g. for constant temperature boundaries $\bar{T} = T_i$ at $r = r_i$ and $\bar{T} = T_i - \Delta T$ at $r = r_o$.

Then the temperature gradient $\beta(r) = -d\bar{T}/dr$. The full temperature $T = \bar{T} + \theta$, so fixed temperature boundaries have $\theta = 0$ at both boundaries. Alternatively, fixed flux conditions have $-\kappa d\bar{T}/dr = F$ a prescribed flux, and then $d\theta/dr = 0$.

Dimensionless equations

Non-dimensionalise with $d = r_o - r_i$ as unit of length, d^2/η as unit of time, $(\Omega\rho\eta\mu)^{1/2}$ as the unit of magnetic field, $\kappa\Delta T/\eta$ as unit of temperature, or Fd/κ in fixed flux case.

$$\frac{E}{Pm}\frac{D\mathbf{u}}{Dt} + 2\hat{\mathbf{z}} \times \mathbf{u} = -\nabla p + \mathbf{j} \times \mathbf{B} + E\nabla^2\mathbf{u} + \frac{ERaPm}{Pr}\theta\mathbf{r}, \quad (5.1.9)$$

$$\frac{\partial \mathbf{B}}{\partial t} = \nabla^2\mathbf{B} + \nabla \times (\mathbf{u} \times \mathbf{B}), \quad (5.1.10)$$

$$\frac{\partial \theta}{\partial t} = \frac{Pm}{Pr}\nabla^2\theta - \mathbf{u} \cdot \nabla\theta + \beta(r)u_r, \quad (5.1.11)$$

$$\nabla \cdot \mathbf{B} = \nabla \cdot \mathbf{u} = 0, \qquad \mathbf{j} = \nabla \times \mathbf{B}. \quad (5.1.12, 13, 14)$$

$\beta(r)$ - Basic state temperature profile. No internal heating assumed here.

Dimensionless parameters

Ekman number $E = \nu/\Omega d^2$, Core value $\sim 10^{-15}$.

Rayleigh number $Ra = \dfrac{g_0 \alpha \beta d^3}{\nu\kappa}$, Core value very large.

Prandtl number $Pr = \nu/\kappa$, Core value ≈ 0.1.

Magnetic Prandtl number $Pm = \nu/\eta$, Core value $\sim 10^{-5}$.

η magnetic diffusivity, ν kinematic viscosity,

κ is the thermal diffusivity, $d = r_o - r_i$.

Even if the molecular diffusivities are enhanced by turbulence $E \sim 10^{-9}$.

Typical simulation values are $Pm = Pr = 1$, $E = 5 \times 10^{-5}$, small but not so small as to make numerical simulation inconvenient.

5.2 Pseudo-spectral method for Boussinesq equations

Poloidal-Toroidal expansion

Poloidal-Toroidal decomposition

$$\mathbf{u} = \nabla \times T\mathbf{r} + \nabla \times \nabla \times P\mathbf{r}. \tag{5.2.1}$$

This guarantees that $\nabla \cdot \mathbf{u} = 0$.

We use (5.1.11) fror the temperature equation, and expand the magnetic field as

$$\mathbf{B} = \nabla \times \mathcal{T}\mathbf{r} + \nabla \times \nabla \times \mathcal{P}\mathbf{r}. \tag{5.2.2}$$

so $\nabla \cdot \mathbf{B} = 0$ exactly.

So we now have 5 scalar functions, P, T, $\mathcal{P}$, $\mathcal{T}$ and θ to integrate forward in time.

The three components of $\mathbf{u}$ and $\mathbf{B}$ have been reduced to two by this expansion.

Expansion in spherical harmonics

Each of these 5 scalars is expanded in spherical harmonics, e.g.

$$P = \sum_{\ell=0}^{\ell=L} \sum_{|m|\leq\ell} P_{\ell m}(r,t) Y_\ell^m(\theta,\phi) \tag{5.2.3}$$

where Y_ℓ^m are the Schmidt normalised spherical harmonics. L is the truncation parameter, typically $L = 128$ or $L = 256$.

Now

$$\hat{\mathbf{r}} \cdot \nabla \times \nabla \times \mathbf{r} P = -r \nabla_H^2 P = \sum_{\ell=0}^{\ell=L} \sum_{|m|\leq\ell} \frac{\ell(\ell+1)}{r} P_{\ell m}(r,t) Y_\ell^m(\theta,\phi) \tag{5.2.4}$$

so each individual component is just multiplied by $\ell(\ell+1)/r$, and the components are not coupled.

Deriving the scalar equations 1.

The radial component of the induction equation (5.1.10) and its curl give two equations for $\mathcal{P}$ and $\mathcal{T}$.

The induction equation is written as

$$(\partial_t - \nabla^2)\mathbf{B} = \mathbf{N_B} = \nabla \times (\mathbf{u} \times \mathbf{B}). \tag{5.2.5}$$

$\mathbf{N_B}$ is the nonlinear term, the other terms are linear. When we insert the expansion (5.2.3) into this and take the radial component, the toroidal term gives nothing, so for each ℓ, m component we can write

$$(\partial_t - \nabla^2)\mathcal{P} = \frac{r}{\ell(\ell+1)}\hat{\mathbf{r}} \cdot \mathbf{N_B}. \tag{5.2.6}$$

So if we can evaluate the ℓ and m components of the nonlinear term, we can use (5.2.6) to timestep $\mathcal{P}$ in a simple way.

Deriving the scalar equations 2.

The radial component of the curl of the induction just gives a very similar equation for $\mathcal{T}$, only the nonlinear term is more complicated.

The same method works for the toroidal components and poloidal components of the velocity.

We write (5.1.9) in the form

$$(\partial_t - Pm\nabla^2)\mathbf{u} = \mathbf{N_u}, \tag{5.2.7}$$

where the Coriolis and buoyancy terms are included in the $\mathbf{N_u}$ term.

We then insert the expansion (5.2.1), and take the radial component of the curl and double curl of this equation.

As with induction equation, the P and T equations separate out, making it convenient to time-step them forward.

Influence matrix method 1.

There is a slight difficulty with the P equation, as this is fourth order in r, so we get two equations

$$(\partial_t - Pm\nabla^2)P = g, \quad -\nabla^2 g = \frac{r}{\ell(\ell+1)}\hat{\mathbf{r}} \cdot \nabla \times \nabla \times \mathbf{N_u}. \quad (5.2.8)$$

However these can be solved simply by using the influence matrix method described in Peyret's book.

Each equation is second order in r. There are two boundary conditions on T, four on P and none on g.

The coupled system for P and g is solved by means of Greens functions with the no-slip condition on P

$$\begin{cases} X\,\bar{P} = \bar{g}, \ (r_i < r < r_o) & \partial r \bar{P} = 0, \ (r = r_i, r_0) \\ Q\,\bar{g} = f, & \bar{g} = 0. \end{cases} \quad (5.2.9)$$

We solve (5.2.9) for $\bar{P}$ and $\bar{g}$ at each time-step.

Influence matrix method 2.

We then solve the time independent equations

$$\begin{cases} X\,P_G = g_G & \partial r P_G = 0 \\ Q\,g_G = 0 & g_G = 1, 0. \end{cases} \tag{5.2.10}$$

$$\begin{cases} X\,P'_G = g'_G & \partial r P'_G = 0 \\ Q\,g'_G = 0 & g'_G = 0, 1. \end{cases} \tag{5.2.11}$$

which can be pre-computed. We then add on the linear combination of P_G and P'_G, $P = \bar{P} + aP_G + bP'_G$, which satisfies the boundary conditions $P = 0$ at $r = r_i, r_o$,

$$\begin{bmatrix} P_G(r_i) & P'_G(r_i) \\ P_G(r_o) & P'_G(r_o) \end{bmatrix} \begin{bmatrix} a \\ b \end{bmatrix} = - \begin{bmatrix} \bar{P}(r_i) \\ \bar{P}(r_o) \end{bmatrix} \tag{5.2.12}$$

P now satisfies the desired boundary conditions $P = \partial r P = 0$ at both boundaries.

Radial dependence

We need to represent the radial dependence numerically. Some codes use a high order finite difference non-uniform mesh over r typically up to 160 points. Other codes expand P_ℓ^m in Chebyshev polynomials.

All differentiation done in spectral space, all nonlinear multiplications in physical space.

At each time-step, the quantities needed to evaluate the nonlinear terms are evaluated on a grid in r, θ and ϕ space. The mesh is used is bigger than the number of spectral coefficients used. If $0 \leq \ell \leq L$, the number of θ points is $3L/2$, a choice known as the de-aliasing rule.

Once the nonlinear terms are evaluated in physical space they can be converted back to spectral space, i.e. expansions in spherical harmonics.

Time-step methods

We can now advance the integration one time-step. The linear terms are advanced implicitly using the Crank-Nicolson scheme, the nonlinear terms explicitly using Adams-Bashforth. A predictor-corrector method is used to choose the time-step.

In practice, it is more convenient to treat some of the linear terms explicitly, i.e. treat them the same way as the nonlinear terms. In particular, the Coriolis terms are usually treated explicitly.

Slowest part of the code is evaluating the Legendre transform to go from the spectral representation to the grid and back. Modern codes have optimised this and so are faster.

A fast Fourier transform can be used in ϕ.

Implementing the magnetic boundary conditions

No-slip boundaries imply $T = 0$, $P = 0$ and $dP/dr = 0$ at the boundaries. Stress-free conditions are also possible.

Insulating magnetic boundary conditions are the most common,

$$\mathcal{T}_{\ell m} = 0 \quad \text{on} \quad r = r_i, r_o, \tag{5.2.13}$$

$$\frac{\partial \mathcal{P}_{\ell m}}{\partial r} - \ell \frac{\mathcal{P}_{\ell m}}{r} = 0 \quad \text{on} \quad r = r_i \tag{5.2.14}$$

$$\frac{\partial \mathcal{P}_{\ell m}}{\partial r} + (\ell + 1) \frac{\mathcal{P}_{\ell m}}{r} = 0 \quad \text{on} \quad r = r_o. \tag{5.2.15}$$

these are derived by matching the field to a potential field inside the inner core and outside the CMB. More complicated options are possible.

5.3 Results from Boussinesq dynamo codes

Results from dynamo codes

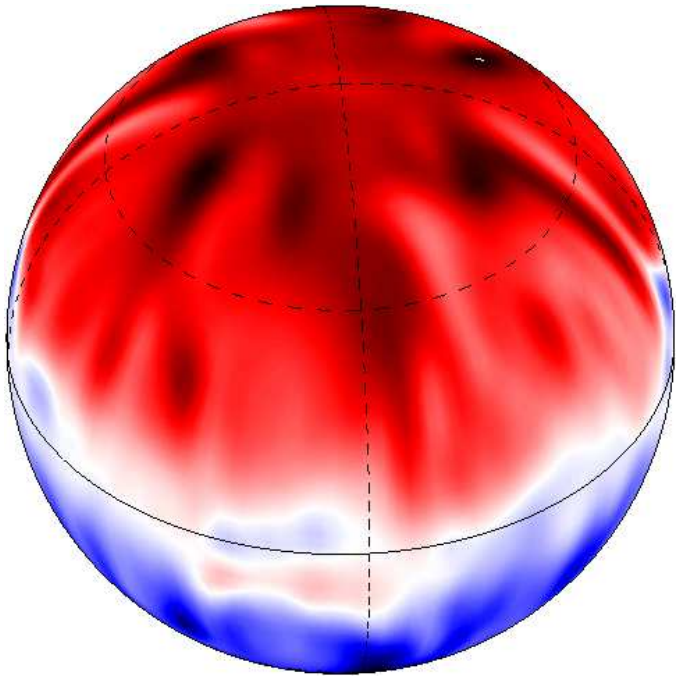

$$Pr = Pm = 1, Ra = 750, E = 10^{-4}.$$

Radial magnetic field snapshot at the CMB

No internal heating. No-slip, fixed temperature, insulating boundaries.

Very dipolar, doesn't reverse. Field slightly weaker at the poles.

Intense flux patches at high latitudes.

Velocity field

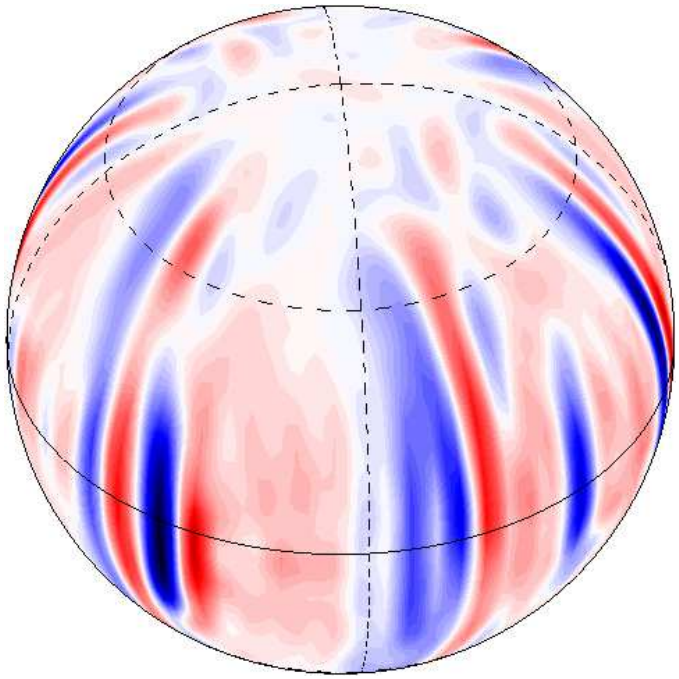

$$Pr = Pm = 1, Ra = 750, E = 10^{-4}.$$

Radial velocity snapshot at
$r = 0.8 r_{CMB}$.
Note the columnar nature of the convection rolls, local Rossby number small.
Intense flux patches at the top of these columnar rolls.
Pattern propagates westward.

Higher local Rossby number

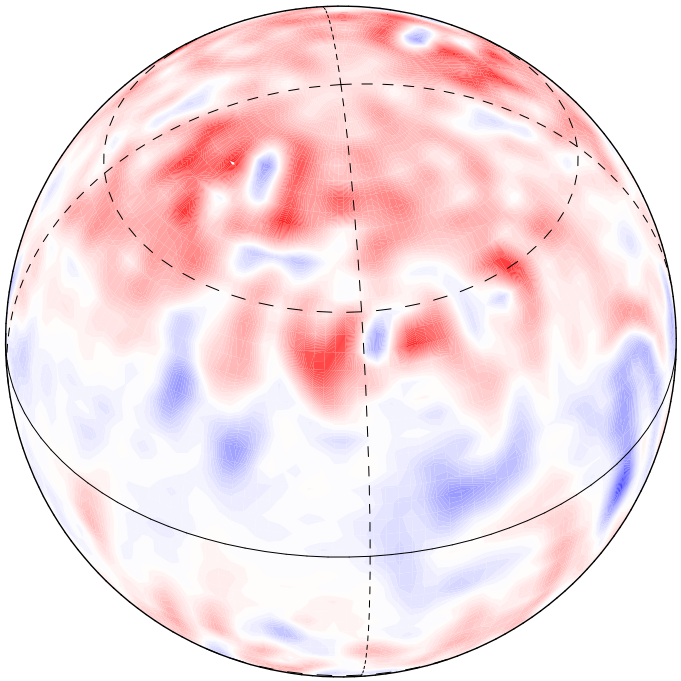

$$Pr = Pm = 0.2, Ra = 750, E = 10^{-4}.$$

Radial magnetic field snapshot at the CMB

Much less dipolar. Field strength is weaker.

This type of dynamo can reverse.

Rossby number is larger, and inertia is playing a significant role.

Flow at higher local Rossby number

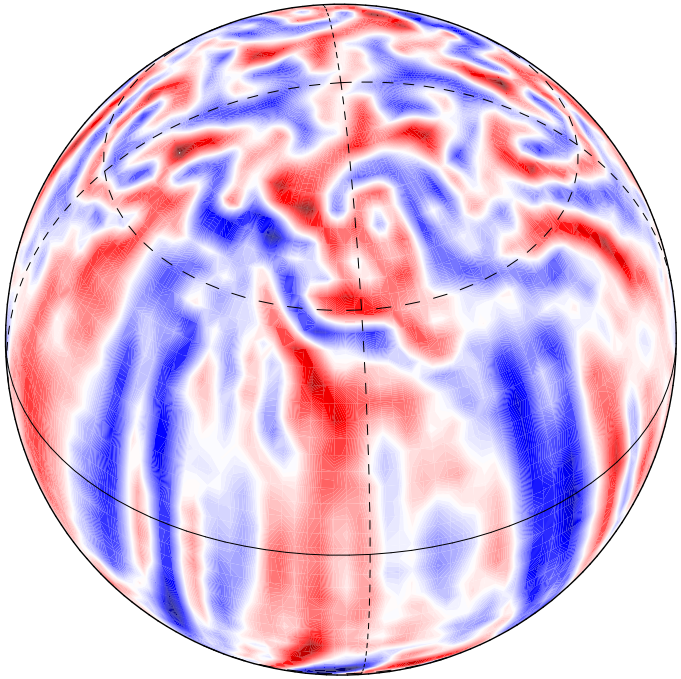

$$Pr = Pm = 0.2, Ra = 750, E = 10^{-4}.$$

Radial velocity snapshot at
$r = 0.8 r_{CMB}$.
More activity near the poles,
less columnar convection rolls.
Between these patterns lies an Earth-like regime.

Variation with Ekman number

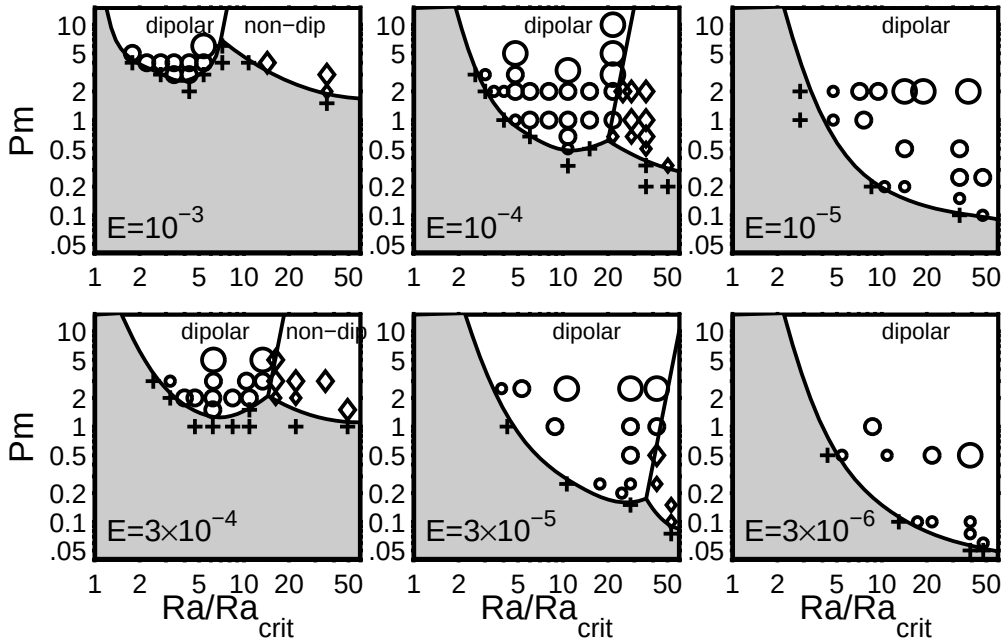

Christensen and Aubert 2006 summarise the dependence on Ekman number E and Pm.

At low E, low Pm dynamos are possible, provided Ra is large enough. Important, as liquid metals have low Pm.

Small E, low Pm dynamo, Flow pattern

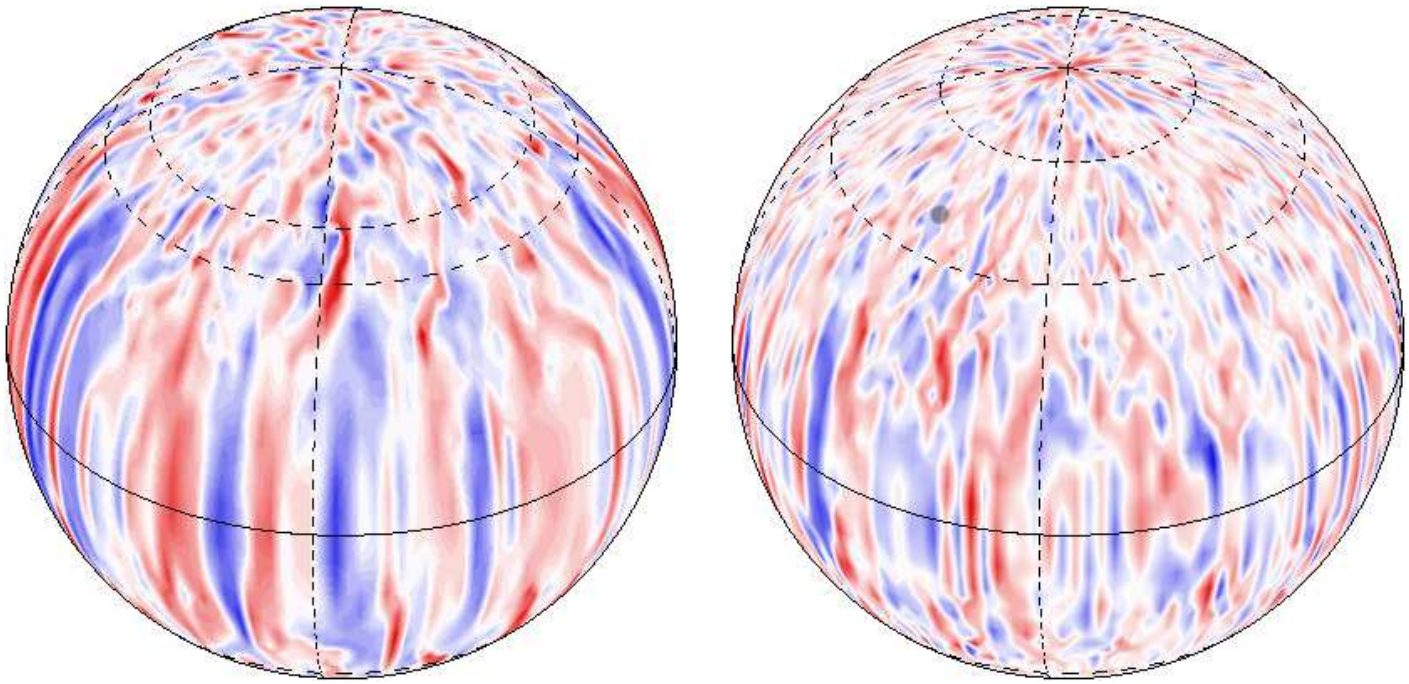

$Pr = 1, Pm = 0.1, Ra = 50 Ra_{crit}, E = 3 \times 10^{-6}$.

Left: radial velocity at $r = 0.5 r_0$. Right: radial velocity at $r = 0.8 r_0$.

At lower E the convective columns are much thinner, particularly further out from the ICB.

Small E, low Pm dynamo, Scale separation

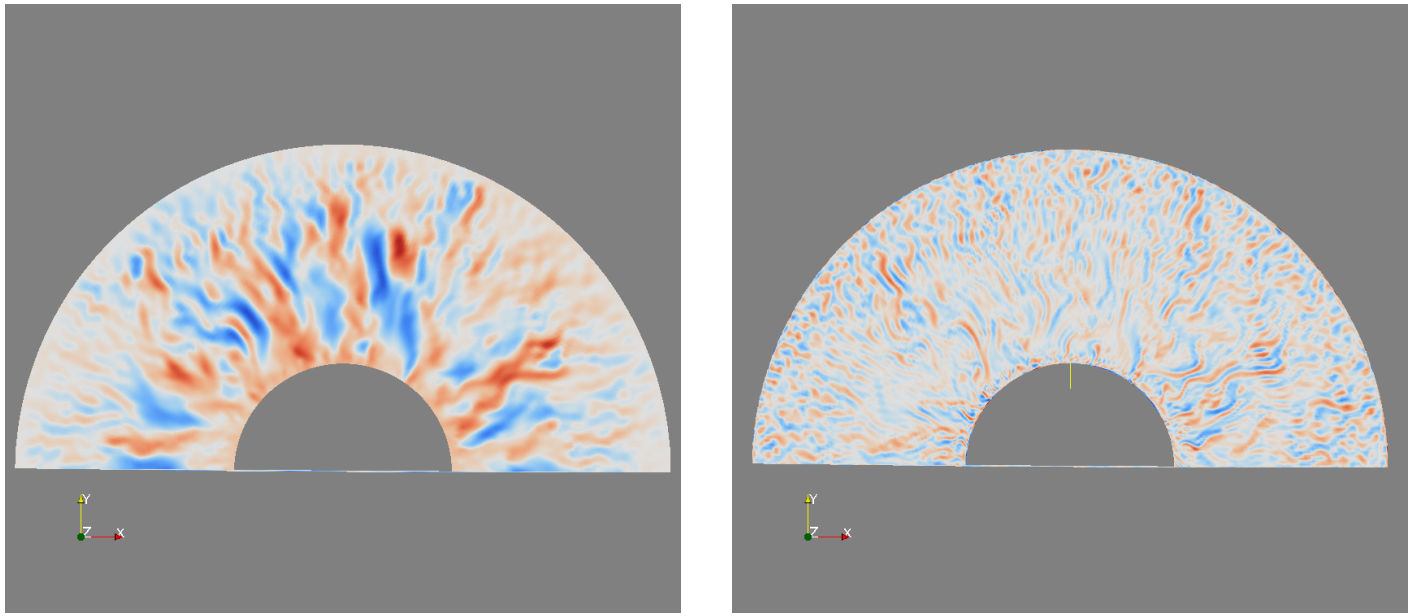

Left: radial magnetic field at $z = 0.2$. Right: vorticity at $z = 0.2$. Notice that the magnetic field is on a much larger scale in these low Pm calculations. Temperature fluctuations on same scale as magnetic field.

Earth-like geodynamo models

Christensen et al. 2010.

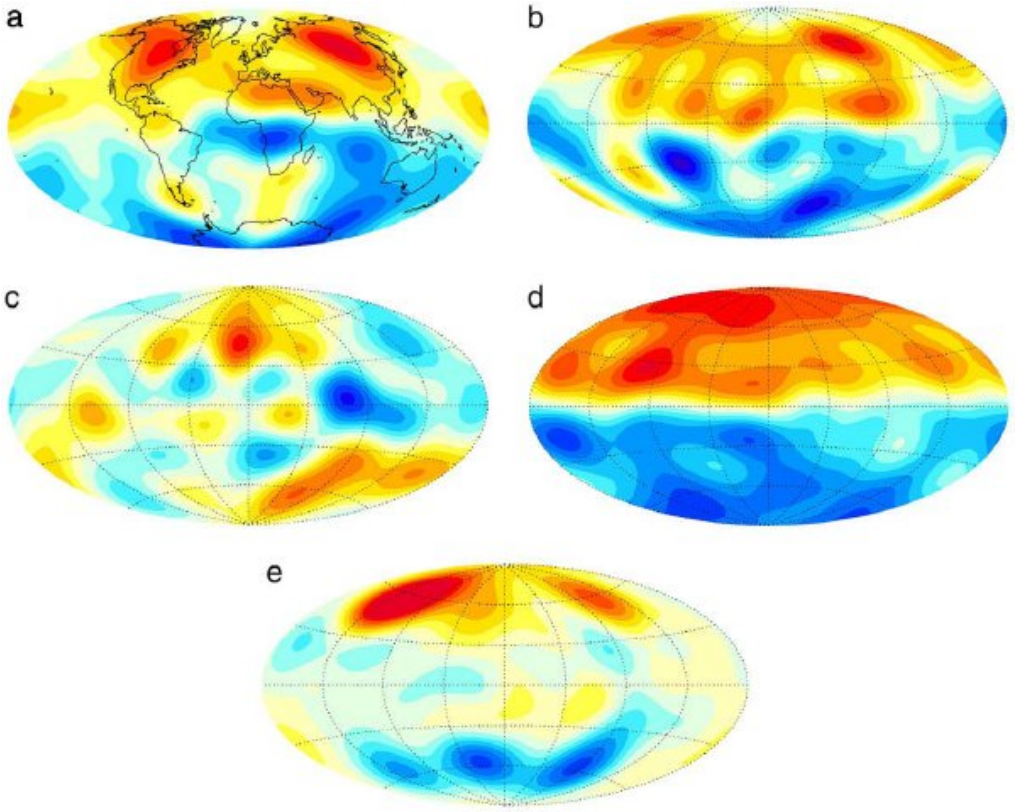

(a) Geomagnetic field. (b) Earth-like geodynamo model with $E = 3 \times 10^{-5}$, $Ra = 3 \times 10^{8}$, $Pm = 2.5$, $Pr = 1$. Zero flux on the outer boundary, compositional driving.
Case (c) is not sufficiently dipolar, (d) is too dipolar, (e) is too strong near the poles.

Wedge for Earth-like geodynamo models

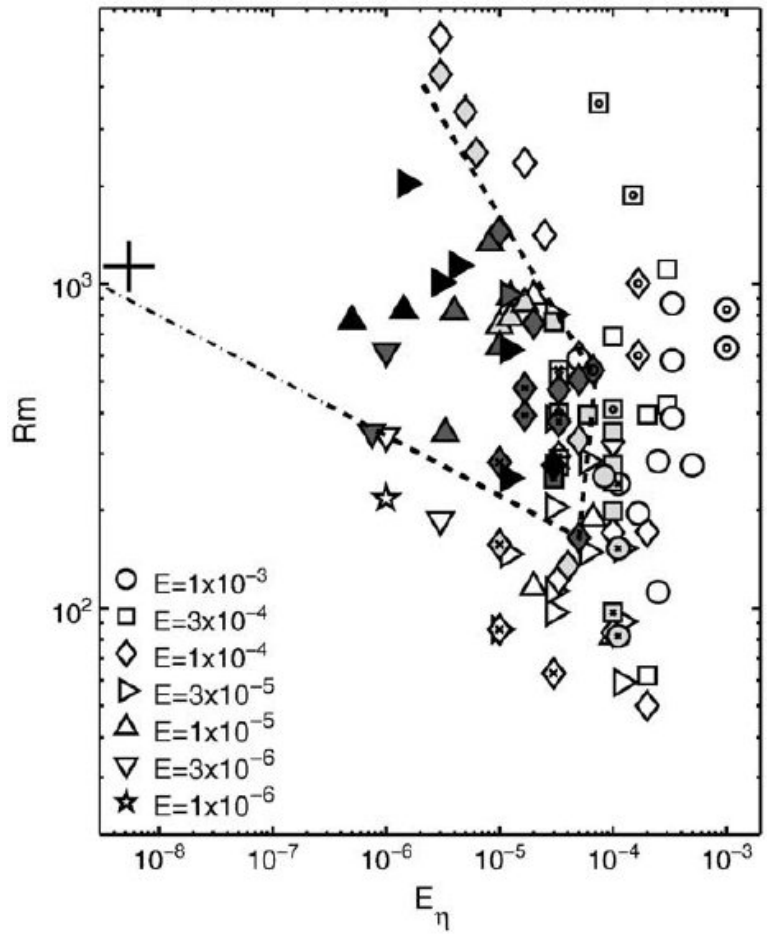

Earth-like geodynamo models have Rm and $E_\eta = E/Pm$ that lie in a particular wedge in the $Rm - E_\eta$ plane. Earth may lie in this wedge too.

Evolution of magnetic energy with time

Sreenivasan and Jones 2011.

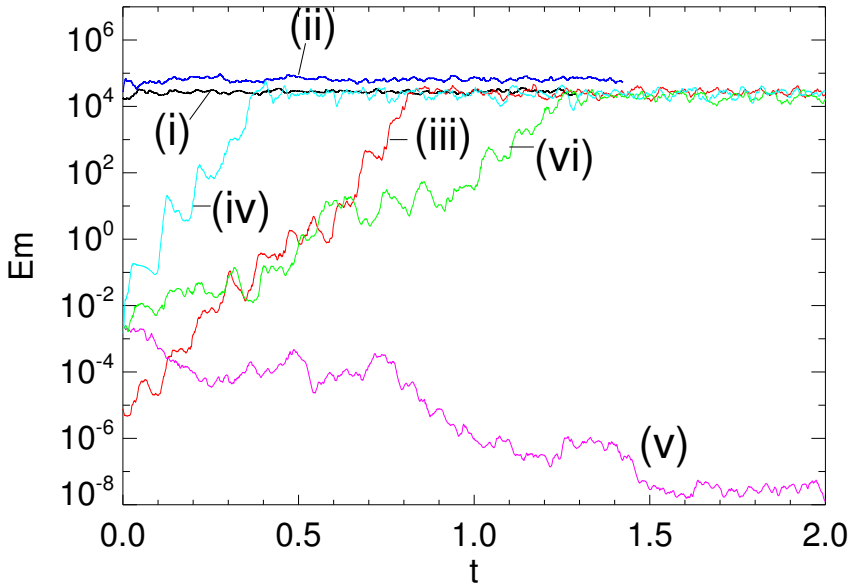

$E = 10^{-4}$, $Pr = Pm = 1$ and stress-free boundary conditions. (i) $Ra = 400$, dipole dominated solution. (ii) $Ra = 600$ strong field dipole dominated solution. (iii) $Ra = 600$, initial small field solution grows into a relatively weak quadrupolar solution. (iv) as case (iii) but with a different small initial field. (v) $Ra = 500$, an initial small field decays away. (vi) $Ra = 550$, an small initial field grows, eventually resulting in a quadrupolar field

Helicity of the strong and weak field solutions

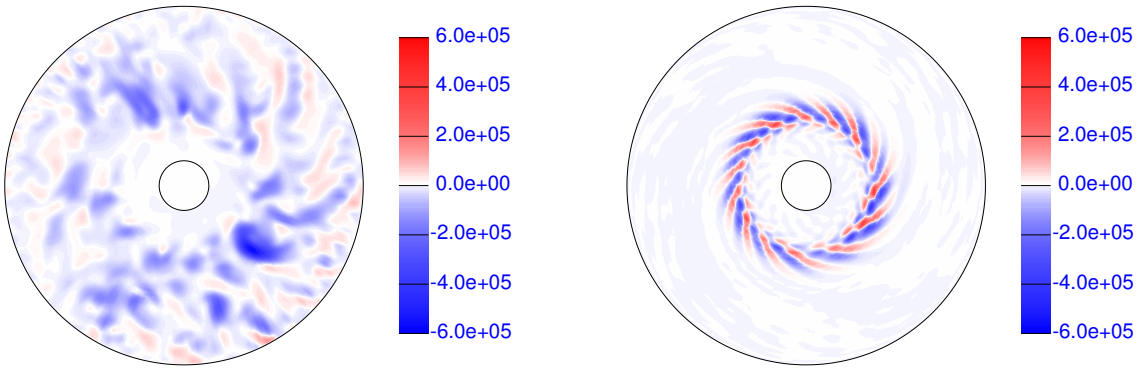

$E = 5 \times 10^{-5}$, $Pr = Pm = 1$, with stress-free boundaries. Helicity is antisymmetric about equator.

Left: is the helicity $\mathbf{u} \cdot \boldsymbol{\zeta}$ for the strong field solution on the plane $z = 0.5$, $Ra = 400$. Right: is the helicity without magnetic field at $Ra = 500$. At $Ra = 500$ an initial seed field decays.

Note that in the pure convection case, there is helicity, but little net helicity. With magnetic field, there is far more net helicity, as predicted by linear theory.

Scaling laws: magnetic field strength

In the Earth's core, magnetic energy is much greater than kinetic energy, so a simple balance as used in astrophysics won't work here.

We start with

Ohmic dissipation + Viscous dissipation = rate of working of buoyancy forces,

The rate of working work done by the buoyancy forces is

$$\int \rho g \alpha T' u_r \, dv$$

which can be written in terms of the heat flux.

Ignore the viscous dissipation and we obtain

$$\int \frac{g \alpha F_{conv}}{c_p} \, dv \sim \int \eta \mu \mathbf{j}^2 \, dv$$

Now need to relate magnetic energy to magnetic dissipation.

Christensen-Tilgner law

The dissipation time is the time taken for the magnetic energy to be dissipated through ohmic loss,

$$\tau_{diss} \int \eta\mu \mathbf{j}^2 \, dv = \int \mathbf{B}^2/2\mu \, dv$$

Equivalently, the magnetic dissipation length

$$\delta_B = \left(\frac{\tau_{diss}}{\eta} \right)^{1/2}.$$

Christensen and Tilgner (Nature, 2004) proposed that

$$\delta_B \sim dRm^{-1/2}$$

mainly on the basis of simulations and laboratory experiments. It also has some theoretical support, because at high Rm flux ropes of this thickness are formed.

Predicted field strength

We now have

$$\eta\mu\mathbf{j}^2 \sim \eta\frac{(\nabla\times\mathbf{B})^2}{\mu} \sim \frac{\eta\mathbf{B}^2}{\mu\delta_B^2} \sim \frac{g\alpha F}{c_p},$$

giving

$$B_* \sim \left(\frac{g\alpha F_{conv}\mu d}{U_* c_p}\right)^{1/2}.$$

With the inertial theory scaling for U_* this gives

$$B_* \sim \mu^{1/2} d^{2/5}\rho^{1/5}\Omega^{1/10}\left(\frac{g\alpha F}{c_p}\right)^{3/10}.$$

Remarkable feature is weak dependence of B on Ω. We are assuming though that the planet is in the rapidly rotating low Ro regime.

5.4 Compressible convection equations

Compressible convection equations 1.

In compressible flow, mass conservation

$$\frac{\partial \rho}{\partial t} + \nabla \cdot (\rho \mathbf{u}) = 0 \qquad (5.4.1)$$

and this replaces $\nabla \cdot \mathbf{u} = 0$, the incompressible flow equation.
The momentum equation is unchanged,

$$\rho \frac{D\mathbf{u}}{Dt} + 2\rho \mathbf{\Omega} \times \mathbf{u} = -\nabla p + \mathbf{g}\rho + \mathbf{j} \times \mathbf{B} + \mathbf{F}_\nu \qquad (5.4.2)$$

except that now the density is no longer constant, but a variable to be determined. $\mathbf{F}_\nu$ is the viscous force. $\mathbf{B}$ is given by (5.1.2), the usual induction equation.
We also need an equation of state giving the pressure in terms of the temperature and density $p = p(\rho, T)$ and an equation for the entropy, $S = S(p, \rho, T)$. We need to use entropy as it appears in the compressible heat transfer.

Compressible convection equations 2.

For a perfect gas,

$$p = R\rho T, \qquad S = c_v \ln \frac{p}{\rho^\gamma} = c_v \ln \frac{T}{\rho^{(\gamma-1)}} + const, \qquad (5.4.3, 4)$$

where R is the gas constant, S is the entropy and c_v and c_p are the specific heats at constant volume and constant pressure, respectively. $\gamma = c_p/c_v$.
Giant planets are not perfect gas, because the hydrogen can be metallic. But the perfect gas case helps for understanding tbe effects of compressibility.
The entropy equation is

$$\rho T \left(\frac{\partial S}{\partial t} + (\mathbf{u} \cdot \nabla) S \right) = \nabla \cdot \rho c_p \kappa_m \nabla T + Q_j + Q_\nu. \qquad (5.4.5)$$

To get to the Boussinesq equation, entropy S is replaced by temperature, ρ and T take their constant reference values and the rate of heating by viscous dissipation Q_ν and ohmic dissipation Q_j are neglected.

Compressible convection equations 3.

This is now a complete set of equations. If we start with an initial condition for all the variables, we use (5.4.1), (5.4.2) and (5.4.5) to evolve ρ, $\mathbf{u}$ and S. Then (5.4.4) determines the temperature T, and (5.4.3) determines the pressure p.

Some numerical simulations of the dynamo equations do work like this, but there are difficulties.

The term $\partial\rho/\partial t$ in (5.4.1) means that sound waves are present in the system. To see this look at small perturbations about the constant entropy, uniform state case.

Sound waves are typically very fast, so we need a very small timestep to integrate the equations, which is not efficient. We use the anelastic equations to avoid this problem.

5.5 Anelastic convection equations

Anelastic models

Compressible systems that are convecting are often close to an adiabatic state.
The anelastic approximation is based on assuming thermodynamic quantities are close to their adiabatic values. Sometimes called thermodynamic linearisation.

$$p = \bar{p}(r) + p', \quad \rho = \bar{\rho}(r) + \rho', \quad T = \bar{T}(r) + T', \qquad (5.5.1)$$

where $\bar{p}$, $\bar{\rho}$ and $\bar{T}$ are (in spherical geometry) functions of radius only, and the primed quantities are small compared to the reference state values.
The reference state is chosen to satisfy the hydrostatic equation $d\bar{p}/dr = -g\bar{\rho}$. For a centrally condensed object where $g = GM_0/r^2$, a polytropic reference state is a popular choice.

Polytropic Reference State

The reference state is then

$$\bar{p} = p_0 \zeta^{n+1}, \quad \bar{\rho} = \rho_0 \zeta^n, \quad \bar{T} = T_0 \zeta, \qquad \zeta = \frac{c_1}{r} + c_0 \tag{5.5.2}$$

where c_1 and c_0 are constants, which satisfies the hydrostatic balance equation.
A polytropic index $n \approx 1/(\gamma - 1)$ ensures that the reference state is close to adiabatic.
Other more complicated, but more realistic models are possible.
If r_i and r_o are the radius of the inner boundary (ICB) and outer boundary (CMB) the r_i/r_o is the radius ratio.

$$N_\rho = \ln\left(\frac{\rho_i}{\rho_o}\right) \tag{5.5.3}$$

measures the density ratio across the spherical shell.

Anelastic approximation 1.

The basic assumption is that the entropy difference across the layer is small, i.e.

$$\frac{S}{c_p} = \epsilon << 1. \tag{5.5.4}$$

Since for perfect gas

$$\frac{p'}{\bar{p}} = \frac{\rho'}{\bar{\rho}} + \frac{T'}{\bar{T}}, \qquad \frac{S}{c_p} = \frac{p'}{\gamma \bar{p}} - \frac{\rho'}{\bar{\rho}}, \qquad \frac{p'}{\bar{p}} \sim \frac{\rho'}{\bar{\rho}} \sim \frac{T'}{\bar{T}} \sim O(\epsilon). \tag{5.5.5}$$

Equation of motion contains terms of $O(\epsilon)$,

$$\bar{\rho}\frac{D\mathbf{u}}{Dt} + 2\bar{\rho}\boldsymbol{\Omega} \times \mathbf{u} = -\nabla p' + \mathbf{g}\rho' + \mathbf{j} \times \mathbf{B} + \mathbf{F}_\nu, \tag{5.5.6}$$

so for consistency, $|\mathbf{u}| \sim O(\epsilon^{1/2})\sqrt{gd}$, where $\sqrt{gd}$ is the free fall velocity across the shell. The Alfvén speed must also be small compared to the free fall velocity.

Anelastic approximation 2.

Now consider mass conservation (5.1.1),

$$\frac{\partial \rho'}{\partial t} + \nabla \cdot (\bar{\rho}\mathbf{u}) = 0, \tag{5.5.7}$$

since $\bar{\rho}$ is independent of time.
Since $|\mathbf{u}| \sim O(\epsilon^{1/2})\sqrt{gd}$, and $\partial/\partial t \sim O(\epsilon^{1/2})\sqrt{g/d}$
and $\rho'/\bar{\rho} \sim O(\epsilon)$, $\partial\rho'/\partial t$ is very small compared to $\nabla \cdot (\bar{\rho}\mathbf{u}) = 0$.

So mass conservation equation is simply

$$\nabla \cdot (\bar{\rho}\mathbf{u}) = 0, \tag{5.5.8}$$

in the anelastic approximation. The sound wave term is removed.

Anelastic approximation 3.

The anelastic equations are now

$$\nabla \cdot (\bar{\rho}\mathbf{u}) = 0, \tag{5.5.9}$$

$$\bar{\rho}\frac{D\mathbf{u}}{Dt} + 2\bar{\rho}\boldsymbol{\Omega} \times \mathbf{u} = -\nabla p' + \mathbf{g}\rho' + \mathbf{j} \times \mathbf{B} + \mathbf{F}_\nu, \tag{5.5.10}$$

$$\bar{\rho}\bar{T}\left(\frac{\partial S}{\partial t} + (\mathbf{u} \cdot \nabla)S\right) = \nabla \cdot \bar{\rho} c_p \kappa_m \nabla T' + Q_j + Q_\nu, \tag{5.5.11}$$

and these, together with the induction equation (5.1.2), can be solved more easily than the full compressible equations.
There are two further modifications to get the system into its most frequently used form.

Entropy diffusion

What is the effect of small scale turbulence on the entropy equation?

In Boussinesq convection, turbulence enhances the molecular diffusion. The **form** of the equation remains the same though. We just have $\kappa_T \nabla^2 T$, with a turbulent value of κ, instead of $\kappa \nabla^2 T$ with a laminar value of κ.

In anelastic convection, it is different. We use the gradient diffusion model, where a small scale $\mathbf{u}^{\mathbf{t}}$ induces a small-scale S'.

Gradient diffusion model

We assume a small-scale turbulence, $\mathbf{u}^t$ which gives rise to a turbulent entropy fluctuation S^t. S^t is forced by the term $\rho(\mathbf{u}^t \cdot \nabla)S$ so its proportional to ∇S. The turbulent entropy flux is then

$$\overline{\rho \mathbf{u}^t S^t} = \mathbf{I}^t = -\rho \kappa_{ij} \frac{\partial S}{\partial x_j}. \tag{5.5.12}$$

We now make the usual assumption that κ_{ij} is an isotropic tensor, $\kappa_t \delta_{ij}$. So

$$\mathbf{I}^t = -\rho \kappa_t \nabla S. \tag{5.5.13}$$

Heat transport with turbulent diffusionl

Enhanced diffusion of entropy also gives a source term of entropy, which turns out to be

$$\sigma^t = -\frac{1}{T}(\mathbf{I}^t \cdot \nabla) T \tag{5.5.14}$$

the only form consistent with energy conservation. So, we get

$$\bar{\rho}\bar{T}\left(\frac{\partial S}{\partial t} + (\mathbf{u}\cdot\nabla)S\right) = \nabla\cdot\bar{\rho}\bar{T}\kappa_t\nabla S + \nabla\cdot\bar{\rho}c_p\kappa_m\nabla T' + Q_j + Q_\nu, \tag{5.5.15}$$

that is turbulent diffusion of entropy and molecular diffusion of temperature.
In compressible convection, the turbulence does not just enhance the molecular diffusion of temperature, it diffuses entropy instead.

Second law of thermodynamics?

Landau and Lifshitz's equation is compatible with the second law of thermodynamics, entropy always increases. Is this true of the turbulence model?
Source is

$$\sigma^t = -\frac{1}{T}(\mathbf{I}^t \cdot \nabla T)$$

so

$$\sigma^t = \frac{1}{T}\kappa_t(\nabla S \cdot \nabla T) \qquad (5.5.16)$$

Entropy gradient and temperature gradient both point outward, so generally OK.

For a stably stratified layer, the entropy gradient and temperature gradient can be opposite, and then entropy diffusion becomes invalid.

Lantz-Braginsky-Roberts approximation

The terms

$$-\frac{1}{\bar{\rho}}\nabla p' + \mathbf{g}\frac{\rho'}{\bar{\rho}}$$

can be rewritten as

$$-\frac{1}{\bar{\rho}}\nabla p' + \mathbf{g}\frac{\rho'}{\bar{\rho}} = \nabla\left(\frac{p'}{\bar{\rho}}\right) - \mathbf{g}\frac{S}{c_p} + \frac{p'}{\bar{p}}\left(\frac{1}{\gamma\bar{p}}\frac{d\bar{p}}{dr} - \frac{1}{\bar{\rho}}\frac{d\bar{\rho}}{dr}\right) \approx \nabla\left(\frac{p'}{\bar{\rho}}\right) - \mathbf{g}\frac{S}{c_p} \tag{5.5.17}$$

the last term vanishing because the reference state is close to adiabatic. The momentum equation can now be written

$$\frac{D\mathbf{u}}{Dt} + 2\boldsymbol{\Omega}\times\mathbf{u} = -\nabla\left(\frac{p'}{\bar{\rho}}\right) - \mathbf{g}\frac{S}{c_p} + \frac{\mathbf{j}\times\mathbf{B}}{\bar{\rho}} + \frac{\mathbf{F}_\nu}{\bar{\rho}}. \tag{5.5.18}$$

Viscous and magnetic terms

The magnetic field **B** and the current **j** are governed by the standard induction equation: compressibility makes no difference. The viscous terms do change,

$$F_{\nu,i} = \frac{\partial}{\partial x_j}\mu\left(\frac{\partial u_i}{\partial x_j} + \frac{\partial u_j}{\partial x_i}\right) - \frac{2}{3}\frac{\partial}{\partial x_i}\mu\frac{\partial u_j}{\partial x_j}, \tag{5.5.19}$$

where $\mu = \bar{\rho}\nu$ is the dynamic viscosity and ν is the kinematic viscosity. The models below are constant kinematic viscosity, but sometime constant dynamic viscosity is used. The viscous dissipation rate is

$$Q_\nu = \mu\frac{\partial u_i}{\partial x_j}\left(\frac{\partial u_i}{\partial x_j} + \frac{\partial u_j}{\partial x_i} - \frac{2}{3}\delta_{ij}\nabla\cdot\mathbf{u}\right). \tag{5.5.20}$$

and the ohmic dissipation rate is

$$Q_J = \mu\eta\mathbf{j}^2. \tag{5.5.21}$$

The anelastic equations are non-dimensionalised in the same way as the Boussinesq equations.

5.6 Pseudospectral method for anelastic convection

Poloidal-Toroidal decomposition

$$\bar{\rho}\mathbf{u} = \nabla \times (\bar{\rho} T)\mathbf{r} + \nabla \times \nabla \times (\bar{\rho} P)\mathbf{r}.$$

This guarantees that $\nabla \cdot \bar{\rho}\mathbf{u} = 0$.
Equations for T and P given by $\hat{\mathbf{r}} \cdot \nabla \times$ momentum equation and $\hat{\mathbf{r}} \cdot \nabla \times \nabla \times$ momentum equation, giving two equations for the two unknowns T and P.
We use (5.5.15) with no temperature diffusion for the entropy equation, and expand the magnetic field as

$$\mathbf{B} = \nabla \times \mathcal{T}\mathbf{r} + \nabla \times \nabla \times \mathcal{P}\mathbf{r}.$$

so $\nabla \cdot \mathbf{B} = 0$ exactly. The radial component of the induction equation and its curl give two equations for $\mathcal{T}$ and $\mathcal{P}$.

Pseudospectral method for solving the equations 2.

We now have 5 equations for the 5 unknowns T, P, S, $\mathcal{T}$ and $\mathcal{P}$, which are closed because of the entropy diffusion ansatz.

Expand all variables as $S = \sum S_{\ell m}(r,t) P_\ell^m(\cos\theta) e^{im\phi}$ and substitute these expansions into the equations. Typically need ℓ from 0-192.

Finite difference non-uniform mesh over r typically up to 160 points. All differentiation done in spectral space, all nonlinear multiplications in physical space.

At each time-step, the quantities needed to evaluate the nonlinear terms are evaluated on a a grid in r, θ and ϕ space. The mesh is used is bigger than the number of spectral coefficients used. If $0 \leq \ell \leq L$, the number of *theta* points is $3L/2$, a choice known as the de-aliasing rule.

Once the nonlinear terms are evaluated in physical spce they can be converted back to spectral space, i.e. expansions in spherical harmonics.

5.7 Anelastic dynamo benchmark

Anelastic Dynamo Benchmark

To test the various codes, the dynamo community ran an anelastic benchmark case to see if they gave the same results.

The case $E = 10^{-3}$, $Ra = 351,806$, $Pr = 1$, $N_\rho = 5$, $r_i/r_o = 0.35$, polytropic index $n = 2$ was selected, as this gives simple solutions and is not very demanding computationally.

The hydrodynamic case with the field switched off was tested, and then magnetic field put back in.

Hydrodynamic benchmark (no magnetic field)

equatorial plane u_r

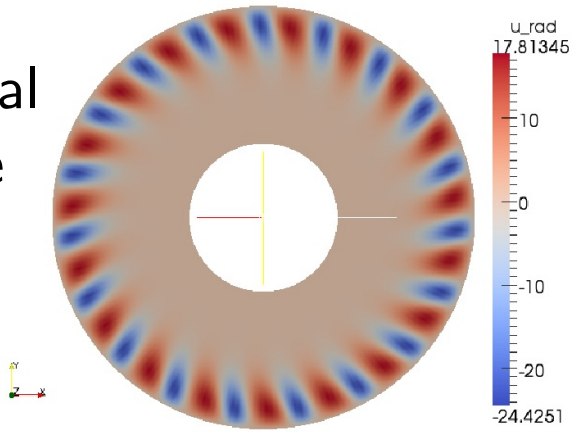

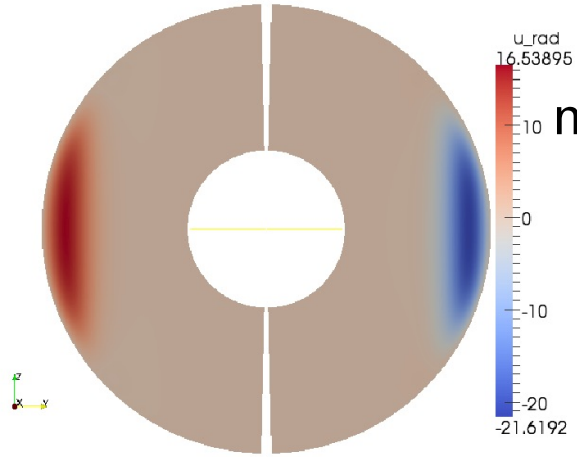

meridional slice u_r

spherical surface entropy $0.93r_0$

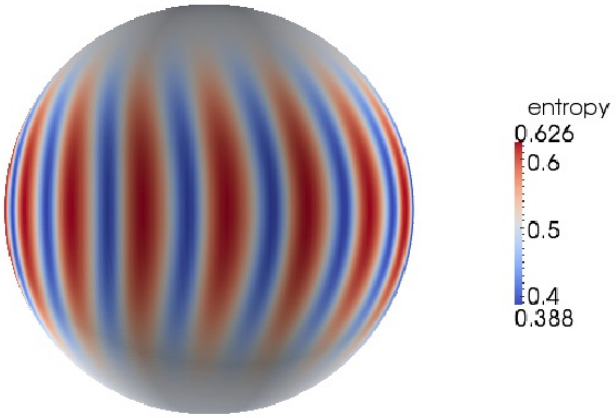

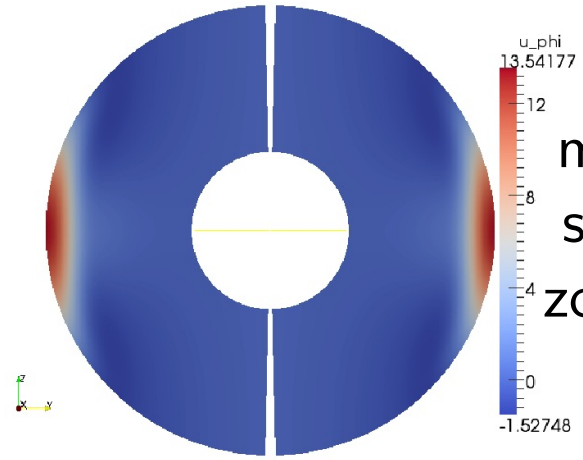

meridional slice zonal u_ϕ

$E = 10^{-3}$, $Ra = 351,806$, $Pr = 1$, $N_\rho = 5$, $\beta = 0.35$, $n = 2$

Solution steady in a drifting frame, has $m = 19$ symmetry. Critical Ra for onset of convection $Ra = 283,175$, with $m = 20$.

Results of the hydrodynamic benchmark

$E = 10^{-3}$, $Ra = 351,806$, $Pr = 1$, $N_\rho = 5$, $\beta = 0.35$, $n = 2$

Code:	Leeds	Glatzmaier	MAGIC
KE	81.8581	81.8335	81.8385
Luminosity	4.19886	4.19886	4.19876
Zonal KE	9.37724	9.37437	9.37514
Meridional KE	0.0220183	0.0220109	0.0220136
Resolution	$128 \times 192 \times 384$:	$121 \times 512 \times 1024$:	$121 \times 192 \times 384$
Timestep	2.5×10^{-6}	5.8×10^{-6}	5×10^{-6}

Agreement to within 0.05%, very satisfactory. Solutions drift eastwards, period 0.0187. Need small timestep.

Steady dynamo benchmark

Steady means steady in a drifting frame. These solutions are very difficult to find. Flow has to have large Rm for a dynamo, but lowish Re to be hydrodynamically stable. Large Pm only possibility, but this is numerically difficult. Needed to compromise on N_ρ and E.

$E = 2 \times 10^{-3}$, $Ra = 80,000$, $Pr = 1$, $Pm = 50$, $N_\rho = 3$, $\beta = 0.35$, $n = 2$

The dynamo is supercritical, $Ra_{crit} = 61,621.682$, with azimuthal wavenumber $m = 10$.

However, the benchmark dynamo has exact $m = 7$ symmetry. Runs did not assume this, but used all wavenumbers, to ensure stability against perturbations of any m.

This compressible dynamo drifts eastwards. The Boussinesq Christensen benchmark drifts westward, and much slower.

Dynamo Benchmark energy

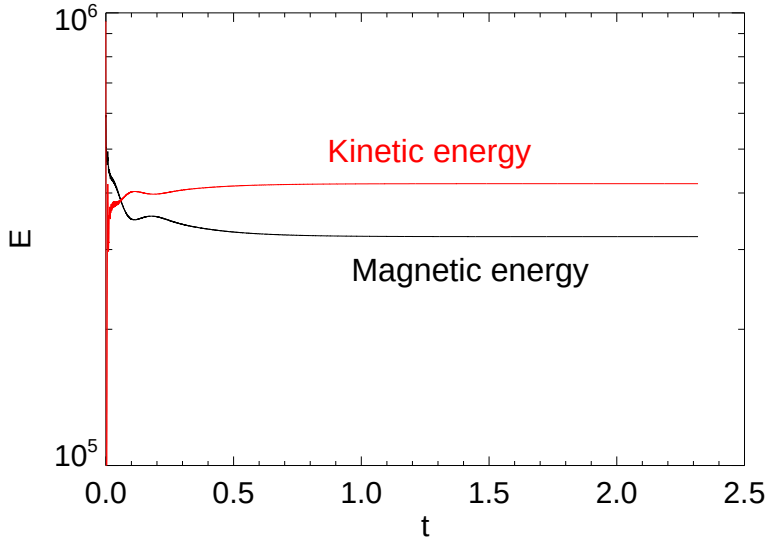

$E = 2 \times 10^{-3}$, $Ra = 80,000$, $Pr = 1$, $Pm = 50$, $N_\rho = 3$, $\beta = 0.35$, $n = 2$

Time here is measured in magnetic diffusion times, so t=2 corresponds to 100 viscous diffusion times. Timestep is 3e-06 (or less) on magnetic diffusion timescale. Fortunately, the solution does not require very high resolution: 64 radial points and 48 X 48 spherical harmonics gives well-resolved solutions.

Steady Dynamo Benchmark Flow

equatorial plane u_r

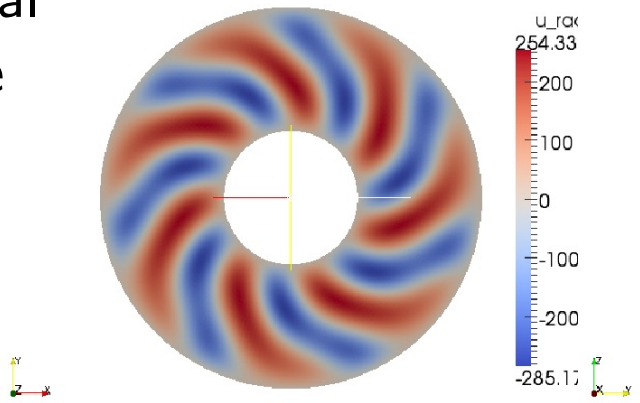

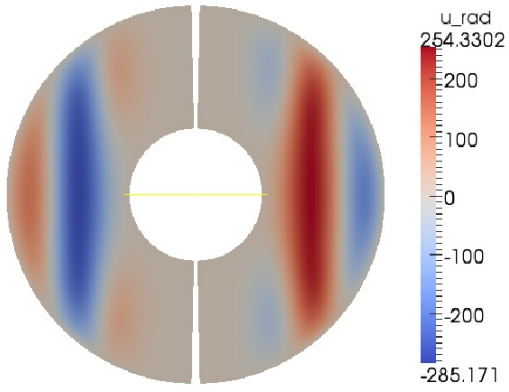

meridional slice u_r

spherical surface entropy $r = 0.86 r_o$

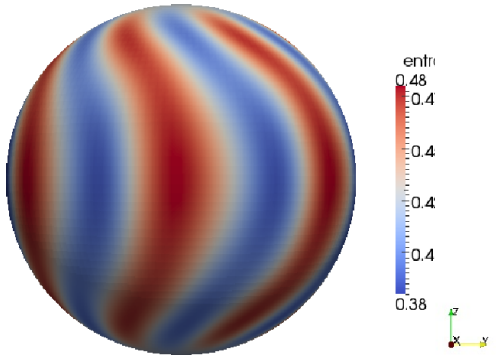

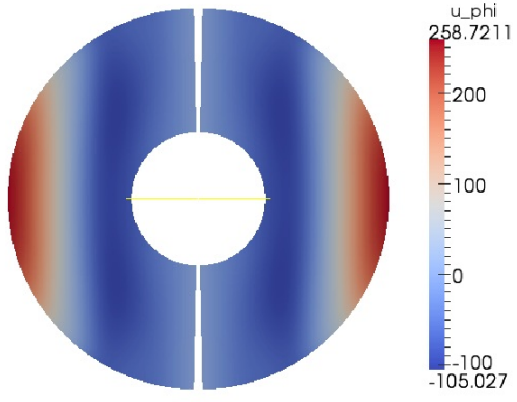

meridional slice zonal u_ϕ

$E = 2 \times 10^{-3}$, $Ra = 80,000$, $Pr = 1$, $Pm = 50$, $N_\rho = 3$, $\beta = 0.35$, $n = 2$

Steady Dynamo Benchmark Field

b_r viewed from N. Pole

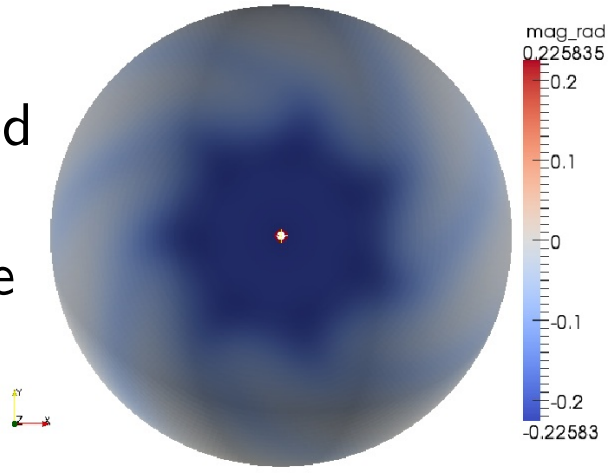

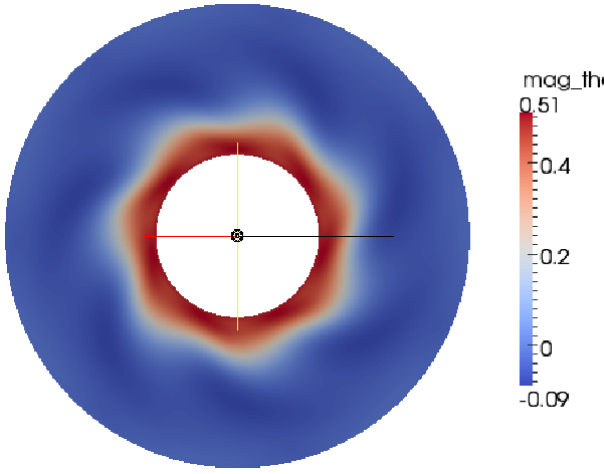

equatorial slice b_θ

spherical surface b_r $r = 0.86 r_o$

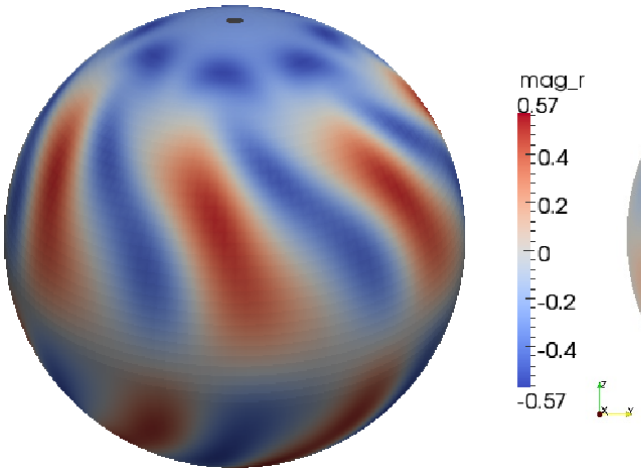

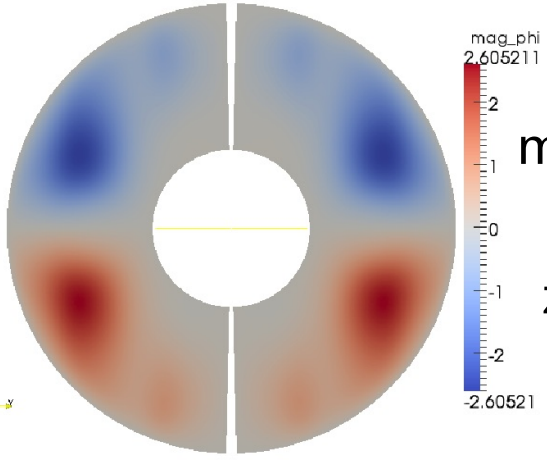

meridional slice zonal b_ϕ

$E = 2 \times 10^{-3}$, $Ra = 80,000$, $Pr = 1$, $Pm = 50$, $N_\rho = 3$, $\eta = 0.35$, $n = 2$

Steady Benchmark Comparisons

Code:	Leeds	Glatzmaier	MAGIC	ASH
KE	4.19407×10^5	4.19390×10^5	4.19438×10^5	4.19106×10^5
ME	3.20185×10^5	3.20083×10^5	3.19749×10^5	3.17330×10^5
Luminosity	11.5030	11.5030	11.5030	11.5033
Resolution	128X144X252:	65X128X256:	65X128X256:	97X256X512
Timestep	10^{-6}	2.1×10^{-6}	10^{-6}	1.4×10^{-6}

Generally OK, though ASH is a bit of an outlier.